Low-Cost Surface Alloying of Brass To Improve Corrosion Resistance In Chloramine-Rich Aqueous Environments

Carol Martinez, Swaroop Kumar Behera , Kaustubh Kishore Rane,
Omid Ghaderi, Mehran Zare, Dave Palmer, Benjamin Church and Pradeep Rohatgi
Department of Materials Science and Engineering, University of Wisconsin–Milwaukee,
Milwaukee, WI 53211, USA

Sara Huerta
Department of Mechanical Engineering, University of Wisconsin–Milwaukee, Milwaukee, WI 53211, USA

ABSTRACT

A cost-effective method of surface alloying brasses (CuZn40 and Bi-alloy C89836) during sand casting was investigated to improve their corrosion resistance. The process involved coating the mold surfaces with slurries containing suspended metal powders before pouring the melt into the sand molds. This casting process allows the internal and external surfaces of a component to be enriched with selected alloying elements, including nickel, leaving the bulk unmodified. Surface-alloyed castings were made both in a laboratory and an industrial setting. The surface-alloyed castings were analyzed using optical and electron microscopy following the casting process. Distinct surface-alloyed layers of average thickness ranging from 100 to 1000 lm were observed on the surfaces of the castings in contact with the molds treated with the slurry containing metal powders. An SEM-EDS analysis confirmed that the surface-alloyed layer was enriched with nickel, ranging from 21 to 62 wt%. Potentiodynamic testing demonstrated that the cast surface-alloyed samples had a higher corrosion resistance than those without surface alloying.

Keywords: brass, surface alloying, in situ, chloramine, corrosion

INTRODUCTION

Brass castings find widespread applications across various industries but often suffer corrosion, particularly in chloramine environments, which are commonly encountered in the water industry. While alloys such as red brass and Monel offer enhanced corrosion resistance compared to CuZn40, they have a higher cost. Brasses that contain zinc concentrations of up to 35 wt% are known as a-brass and have a face-centered cubic crystal structure. There is also a zinc-rich b-brass containing about 45–50% Zn with a body- centered cubic crystal structure. Duplex a ? b brasses (with about 35–45% Zn), having a combination of both crystal structures, are relatively cheap and display better mechanical strength than a-brasses, but the zinc-rich b phase has a higher tendency to dezincification corrosion.[1] The zinc tends to pass into the corrosive medium, leading to copper appearing on the brass surface in the form of a fine-grained porous layer with poor mechanical proper- ties.[1,2] A major application of brass is in drinking water distribution systems for tube fittings, valves, and faucets. Most commercial brasses for drinking water distribution have $\alpha + \beta$ structure due to their improved mechanical properties and easy forming capability.[1]

In water industry applications, the surfaces of components are exposed to chlorides or chloramines in water.[3–5] This is a major concern since chlorine and chloramine in the water accelerate corrosion, leading to mechanical failure.[2] Additionally, this can be a costly problem due to the frequent need for replacement and maintenance of the part. Copper alloys have been researched and developed for many years; however, there are copper alloys that exhibit higher corrosion resistance than CuZn40. Red brass has a higher copper content than CuZn40, making it more expensive, but it has the benefit of increased corrosion resistance. Monel is a copper-nickel alloy that demon- strates much higher corrosion resistance compared to CuZn40 and red brass. It was found that the service life of red brass and Monel exceeded that of CuZn40 in chlo- ramine environments.[6] However, both red brass and Monel are much more expensive compared to CuZn40 alloys.

This exposure of brass components to corrosive aqueous and atmospheric conditions leads primarily to the degradation of their surfaces.[7] This suggests that one can focus on improving the properties of the surface of the material and leave the bulk unmodified since the properties of the component surface have major impacts on the life of components used in the water industry.[8] Since corrosion and wear are primarily a surface phenomenon, extensive research has been done on coatings and surface alloying techniques. Surface alloying involves the deposition and mechanical bonding of additional metals or alloys on the surface of the metallic base alloy component.[7] There are various methods for achieving surface alloying, including carburizing, nitriding, tungsten-inert gas heat treatment, and plasma deposition. A crucial aspect that makes surface alloying an attractive technique is the formation of a layer as a part of the bulk material and the ability to control the thickness of the surface-alloyed layer. This enables various materials to be surface alloyed with different elements using different techniques.[7,9]

The research described in this paper utilizes conventional sand casting to alloy the surfaces of brass castings and enrich them in elements that reduce the corrosion of castings. Sand casting is a lower-cost method of surface alloying compared to other surface alloying methods for modifying the surfaces of the castings, which are also energy-intensive, expensive, and require a line of sight; therefore, it is not suitable for surface alloying of interior surfaces of hollow components. This work aims to surface alloy brass castings using a cost-effective engineered coating sand casting technique to enhance the corrosion resistance of brass in chloramine- containing water. Since brass is a commonly used alloy in the water industry, the internal surface of the brass must resist the chloramine-containing water. This technique has been demonstrated for surface alloying the internal surface of a low-carbon steel casting with elements such as chromium and nickel to enhance the corrosion resistance of mild steel castings.[10] The goal of this work is to prove the feasibility of surface alloying components of yellow brass (CuZn40) and Bi-alloy (C89836) during sand casting to improve their corrosion resistance. This technique can be beneficial for water industries due to the widespread use of sand casting to make water industry components and the possibility of improvement of corrosion properties just on the surface of brass without the need for alloying the whole component.

EXPERIMENTAL PROCEDURE

The primary experiments to test the viability of the surface alloying process were done at the University of Wisconsin- Milwaukee (UWM) Foundry Lab to demonstrate surface alloying at a laboratory scale. Figures 1 and 2 show the sand casting process used for surface alloying at the UWM foundry. The sand molds were made from chemically bonded silica sand using a phenolic urethane no bake binder system. The mold cavities were coated with a zirconia-based refractory wash and then with a slurry containing metal powders for surface alloying. The refractory wash was applied to prevent any possible reaction between sand and melt, inhibit sand inclusions in the casting surface, and provide a smooth base for applying the metal-binder slurry. The molds were then dried in a low-temperature oven at 200 °C for 2 h to remove volatile compounds and water from the slurry, as well as preheating the mold for the casting process.
The slurry utilized in the process was made of a combination of alloying powders, and two different water-based binding media, including a proprietary two-part suspending media (from Vibrantz Technologies) and a commercial mold coating without refractory particles (REFCOBAR 1010, from Refcotec)

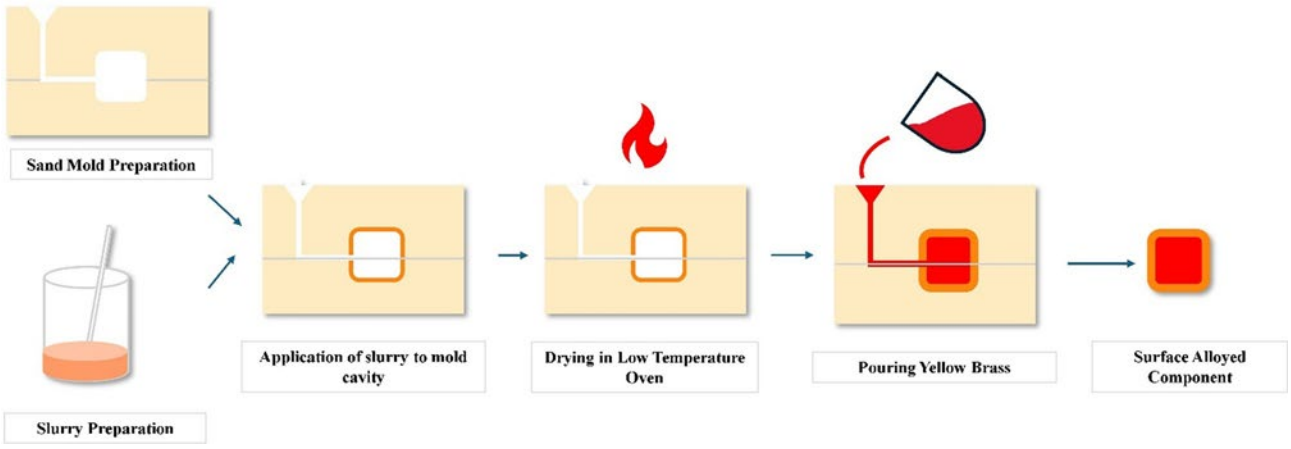

Figure 1. A schematic of mold making, slurry application, and casting process for the surface-alloyed samples.

Based on our previous work done with steel, water-based binders work well for this pro- cess.[7,9,10] The flowability of the metal-binder slurry and its adhesion to mold walls were important aspects of the slurry preparation. The nickel (Ni) and Cu powders were the primary alloying elements utilized in this study. The Ni, as in the case of Monel alloys, improves the corrosion resistance in chloramine environments.[6] The alloying powders were procured from high-purity grade suppliers, and the particle sizes and purities are listed in Table 1. The slurry was applied using either flow coating or brush application. While spraying is a viable option, factors such as particle size, density of alloying powders and the viscosity of the slurry need to be optimized before implementing it. Thus, spraying was not tested as a slurry application method in this study.

Figure 2. Mold with surface alloying slurry coated on mold cavity prepared at the UWM Foundry Lab.

Table 1. Particle Size and Purity of the Alloying Powders Used in the Study

Alloying Element	Particle Size	Purity (%)
Cu	–200 mesh	99
Ni	–100 mesh	99.9
Cu-Sn (90–10)	–200 mesh	99
Al	200 mesh	99

At the UWM Foundry Lab, 3.5 lbs. of C89836 brass was melted at 1150 °C in an induction furnace. A layer of borax was added as flux to prevent the evaporation of zinc from the melt. The melt was cast into slurry-coated molds, and the cast samples were allowed to cool to room temperature before small coupons were cut for metallographic examination.

INDUSTRIAL FOUNDRY TRIALS

Sand cores made from chemically bonded silica sand were obtained and coated with a refractory wash (Technikoat) provided by the partner foundry. The coated cores were left to air-dry to prepare the surface for the application of slurry, which contained metal powders for surface alloying. The slurry containing metal powders was applied and dried at room temperature to remove volatiles and moisture. Combinations of Ni, Cu, and Al powders were added to the binder in varying percentages to form the slurry. The cores were placed in green sand molds at room temperature, and the molds were cast at the partner foundry. The C89836 melt temperature was approximately 1100 °C prior to pouring the melt into the molds, and Cu-P shots were added to the ladle before pouring to remove any dissolved gases. The castings were then allowed to cool, and small coupons were cut and prepared for metallography. A total of 50 samples were cast at the partner foundry (Figure 3).

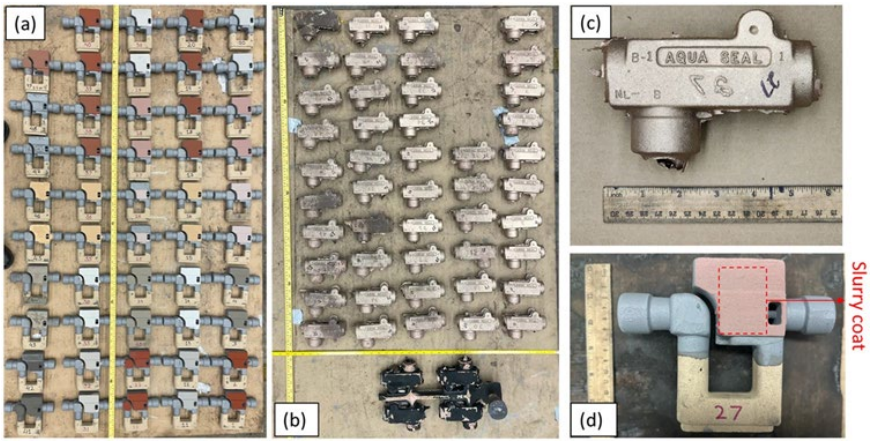

Figure 3. (a) Sand cores coated with alloying powder slurry, (b) surface-alloyed castings obtained from the partner foundry, closeups of the (c) final casting and (d) slurry-coated sand core.

The two control samples were coupons of CuZn40 and C89836 alloys. The CuZn40 was obtained from a supplier with a composition of 60/40 Cu-Zn. A partner foundry provided the C89836 brass. The composition of these alloys is given in Tables 2 and 3.

Table 4 details the processing parameters for all four samples discussed in this paper.

METALLOGRAPHIC PREPARATION

After the casting process was completed, small coupons were cut from the castings and prepared for metallographic examination. The samples were cut using a bandsaw and subsequently mounted utilizing conductive phenolic resin. The specimens were ground with SiC abrasive papers and polished with 1-um alumina suspension.

To reveal the difference between the base metal and surface-alloyed layer, Copper No. 2, a ferric chloride-based etchant, was employed. The etching time was approximately five seconds.

Table 2. Composition of CuZn40

Cu (wt%)	Zn (wt%)
60	40

CHARACTERIZATION

Scanning electron microscopy (SEM) imaging (JEOL 6460LV) and X-ray diffraction (XRD) analysis (Bruker D8 Discover with Cu anode), with parameters shown in Table 5, were used to examine the microstructure and phase composition. To confirm the presence of alloying elements in the surface-alloyed layers, energy-dispersive spectroscopy (EDS) was employed with methods such as point and ID, line papping, and area mapping to identify the distribution of the alloying elements. Point and ID was used to quantitatively measure the weight % of alloying elements in the surface-alloyed layer and base metal. Area mapping was used to observe the distribution of alloying elements, while line scanning was used to show the variation of alloying elements along a line through the surface- alloyed layer into the base metal. The SEM-EDS measurements were taken using an accelerating voltage of 15 kV and a spot size of 50.

Potentiodynamic tests were carried out using Bio-logic Science Instruments' SP-200 Potentiostat using an EC lab software to measure corrosion resistance. A conventional three-electrode glass cell consisting of a sample coupon as the working electrode, platinum mesh, and Ag/AgCl in3.5M KCl was used as counter and reference electrodes, respectively, as shown in Figure 4. All potentials were measured against the reference electrode. Prior to all electrochemical measurements, the working electrode was immersed in tap water (2 ppm chloramine) for 24 h to attain a stable corrosion potential (OCP). Tests were performed in tap water at 25 °C. Potentiodynamic resistance experiments were done from –0.25 to ?0.25 V versus E_{corr} at the scan rate of 10 mV/min. Tafel plots were used to obtain the corrosion current (I_{corr}) (Table 6).

Table 5. The XRD Parameters Used for Sample Analysis

2h	20°–90°
Voltage	40 V
Amperage	40 Amp
Filter	Ni
Ka_1	1.5406
A°	

Table 3. Composition of C89836 Brass

	Cu	Pb	Sn	Zn	Fe	P	Ni	Al	Bi	S	Sb	Si
Min (wt%)	87	–	4.0	2.0	–	–	–	–	1.5	–	–	–
Max (wt%)	91.0	0.25	7.0	4.0	0.35	0.06	0.9	0.005	3.5	0.08	0.25	0.005
Measured	89.1	0.020	4.46	4.61	0.056	0.025	0.825	0.003	1.70	0.007	0.044	0.00

Table 4. Selected Samples and Their Experimental Parameters

Sample	Alloying element	Base alloy	Pouring temperature (°C)	Binder	Casting location
S1	Ni	C89836	1150	Mold Coating (Refcobar 1010)	UWM Foundry Lab
S2	Cu–Al (3:1)	CuZn40	1200	Suspending Media (Vibrantz)	Partner Foundry
S3	Ni	C89836	1100	Mold Coating (Refcobar 1010)	Partner Foundry
S4	Cu–Ni (1:1)	C89836	1100	Suspending Media (Vibrantz)	Partner Foundry

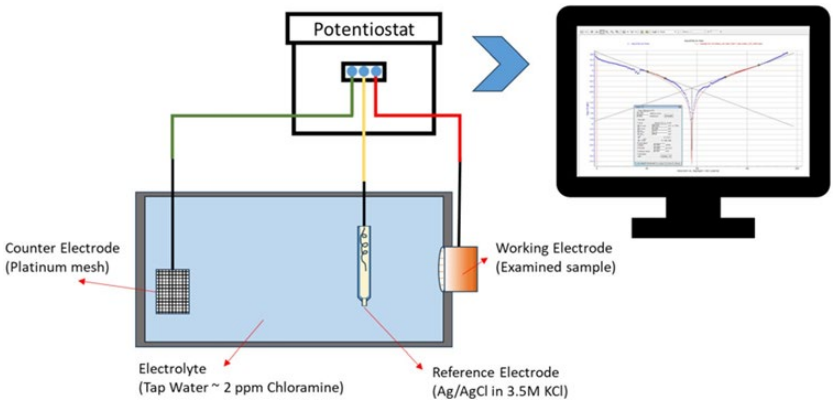

Figure 4. Corrosion setup for potentiodynamic testing.

Table 6. Average Thickness of the Surface-Alloyed Layer in the Four as-Cast Samples

Sample	Average Thickness Of The Surface-Alloyed Layer (□m)
S1	1500
S2	50
S3	175
S4	300

3.5M KCl was used as counter and reference electrodes, respectively, as shown in Figure 4. All potentials were measured against the reference electrode. Prior to all electrochemical measurements, the working electrode was immersed in tap water (2 ppm chloramine) for 24 h to attain a stable corrosion potential (OCP). Tests were performed in tap water at 25 °C. Potentiodynamic resistance experiments were done from -0.25 to ?0.25 V versus Ecorr at the scan rate of 10 mV/min. Tafel plots were used to obtain the corrosion current (Icorr) (Table 6).

RESULTS AND DISCUSSION

MICROSCOPY AND COMPOSITIONAL ANALYSIS

Optical micrographs of the cross section of the surface-alloyed as-cast samples were obtained. The primary phases observed in duplex brasses are the α-phase and the β- phase; the a phase is rich in copper, while the β phase is rich in zinc.1 Figure 5a shows the Widmanstätten-like microstructure of the control sample of CuZn40. The microstructure of C89836 revealed after etching with Copper No.2 is shown in Figure 5b. C89836 has a higher copper content than CuZn40, which contributes to its longer component life in chloramine environments.6 However, the downside of this additional copper is its higher cost, as the price of copper continues to rise. The image analysis of these microstructures was done to measure the average thickness of the surface-alloyed layer.

Figure 6 shows a portion of the surface-alloyed layer in sample S1 with nickel as the surface alloying element and C89836 as the base metal. This sample demonstrates two distinct regions: the surface-alloyed layer and the base metal, which are in continuous contact with each other. The phase diagram of the Cu-Ni system shows that nickel has complete solubility in copper and forms a single-phase a structure.11 Figure 7 illustrates the total thickness of the surface-alloyed layer and the results of multiple EDS characterizations of samples conducted for compositional analysis of sample S1. The surface-alloyed layer has a maximum thickness of 1500 lm with relatively uniform thickness; however, some porosities are also observed. The concentration of Cu, Sn, Ni, and Zn in the base alloy and the surface-alloyed layer were examined and are shown in Table 7. The concentration of Ni was observed to be higher in the surface-alloyed layer, as seen in spectrums 1 and 2, compared to the base alloy in spectrums 3 and 4. A line scan of the concentration of the alloying elements showed a similar trend, with the intensity of Ni dropping sharply on crossing the interface between the surface-alloyed layer and the base metal, as seen in Figure 8. A small concentration of Ni, 1.6 – 1.8 wt% was observed in the base material due to the Ni present inherently in C89836. The concentration of Zn and Sn remained relatively constant in all areas.

Sample S2 was cast with CuZn40 as the base alloy, and Cu- Al powders were used for surface alloying since aluminum has several advantages, including improvement in corrosion resistance, lower melting point, and low cost com- pared to Ni. The addition of Al has been reported to

progressively improve the corrosion resistance of brasses in terms of reduced depth of corrosion and rate of corrosion.12 Aluminum, due to its lower melting point (compared to base metal), is expected to melt more readily when it comes in contact with the melt. Sample S2 showed a fairly continuous surface-alloyed layer with an average thickness of about 50 □m, as shown in Figure 9. The surface-alloyed layer did not show any measurable porosity, and a single- phase region is observed in the surface-alloyed layer, while two distinct phases are seen in the base alloy. The chemical composition of the cross section was determined at three locations, and a decrease in the weight percentage of Cu in the surface-alloyed layer was observed as it moved toward the base alloy, as shown in Table 8. Aluminum concentrations remained close to 1 wt% at the surface, and no Al was observed in the base metal.

Sample S3 was cast in C89836 at a partner foundry with pure Ni as the surface alloying element. The thickness of the surface-alloyed layer observed in this case was approximately 150–200 □m, as shown in Figure 10. The primary difference between samples S3 and S1 is the significantly higher nickel (Ni) weight percentage in the surface-alloyed layer of sample S3. Although sample S1 had a thicker surface-alloyed layer, sample S3 had a thinner layer with a higher Ni concentration.

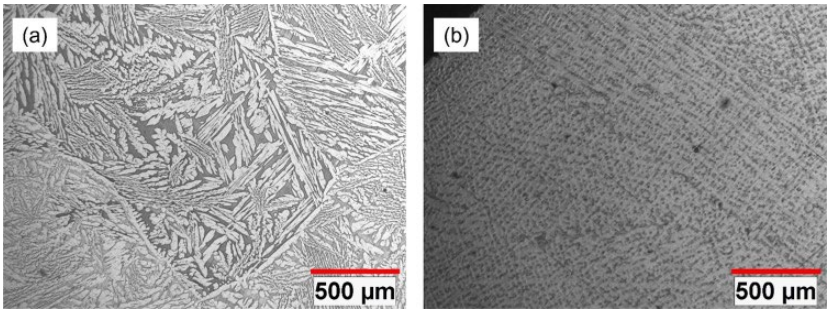

Figure 5. Microstructures of control samples at 503–(a) CuZn40 brass, (b) C89836 brass.

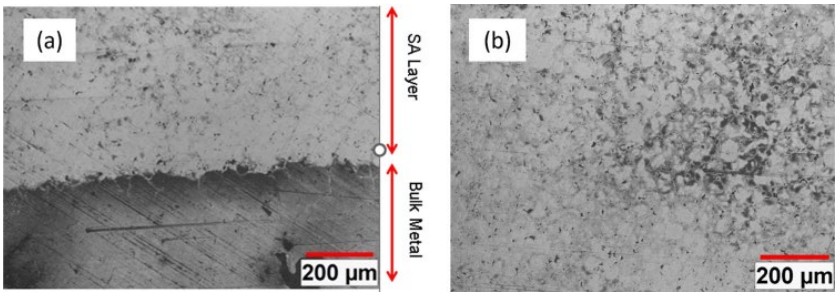

Figure 6. Unetched micrographs of sample S1 showing (a) the boundary between the surface-alloyed layer and base metal at 100x magnification and (b) the surface- alloyed layer at 100x magnification.

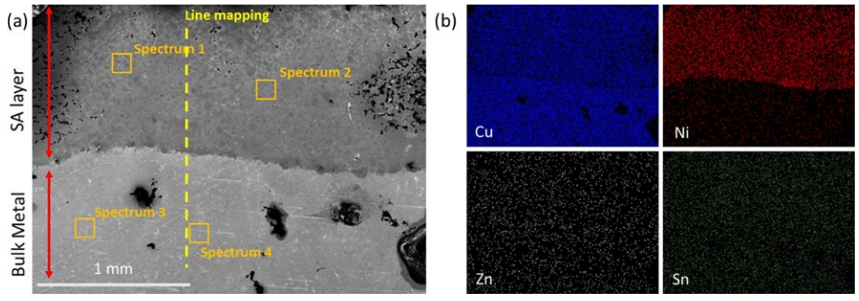

Figure 7. An EDS analysis of Sample S1 determined the distribution of the alloying elements (a) point and line analysis, (b) area mapping of the surface-alloyed layer and base metal.

This discrepancy may be attributed to differences in pouring temperature and heat flow from the mold when the melt was poured in the industrial foundry, resulting in a different cooling rate compared to sample S1, which was cast in the UWM Foundry Lab. As shown in Table 9, the Ni weight per- centage in the surface-alloyed layer of sample S3 was 62 wt%, whereas it was nearly 1 wt% in the base metal. In contrast, the Ni concentration in the surface-alloyed layer of sample S1 ranged from 20 to 28 wt%. The concentration of Zn was higher in the base metal of sample S3 compared to the surface-alloyed layer, which is similar to what was observed in other samples as well.

Table 7. Alloying Elements Present in the Surface-Alloyed Layer and Base Metal of Sample S1

Spectrum	Ni (%wt)	Cu (%wt)	Zn (%wt)	Sn (%wt)
Spectrum 1	21.86	71.15	3.00	3.98
Spectrum 2	28.26	64.12	3.58	4.03
Spectrum 3	1.65	89.47	3.96	4.92
Spectrum 4	1.81	89.71	4.49	3.98

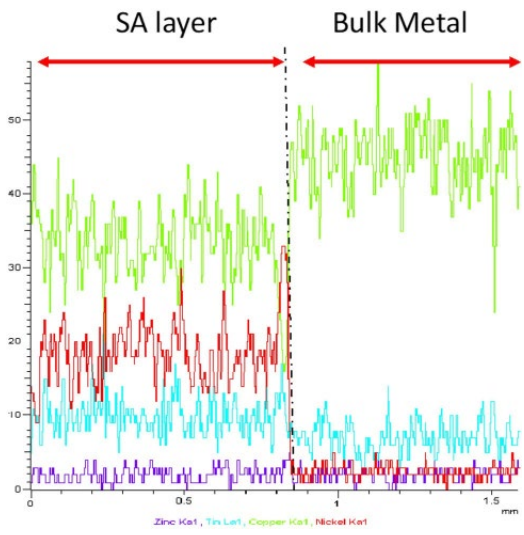

Figure 8. Line scan of S1 showing Zn (purple), Sn (cyan), Cu (green), and Ni (red) across the interface between the surface-alloyed layer and base metal.

Sample 4 was poured using C89836 alloy into a mold that had Cu and Ni powders mixed in a 1:1 ratio in the applied slurry. The Cu–Ni mixture was used to facilitate the melting of nickel in the slurry at a reduced temperature. Figure 11a shows the microstructure of Sample 4. Fig- ure 11b is a composite image of optical micrographs stit- ched together to display the entire length of the surface-alloyed region on the sample, along with an area scan analysis of the cross section of the surface-alloyed casting. This figure demonstrates that the surface-alloyed layer was continuous over a considerable length and enriched in Ni. The Ni concentration in the surface-alloyed layer was higher than in the base alloy. In all experiments in this study, the surface-alloyed layer formed during casting appeared to be integrally bonded with the casting. This differs from coatings, which exist as separate layers that can peel off.

Table 8. Alloying Elements Present in the Surface-Alloyed Layer and Base Metal of Sample S2

Spectrum	Cu (%wt)	Zn (%wt)	Al (%wt)
Spectrum 1	90.47	8.10	0.81
Spectrum 2	69.36	28.37	1.04
Spectrum 3	66.08	33.43	0.00

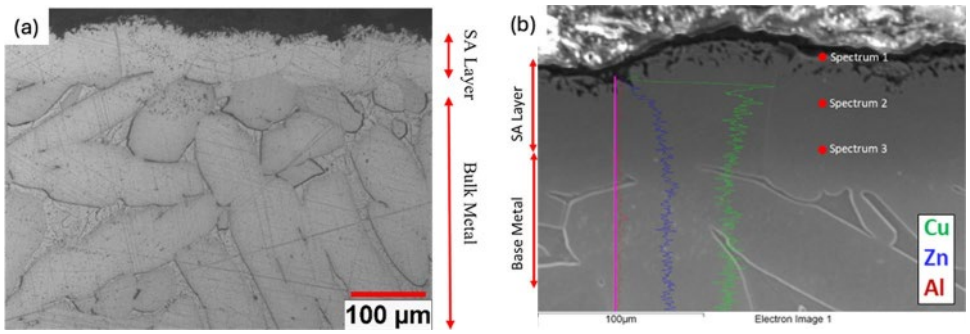

Figure 9. (a) Optical micrograph of sample S2 at 2003, (b) SEM micrograph showing line scan and point analysis of sample S2 showing alloying elements Cu (green), Zn (blue), and Al (red).

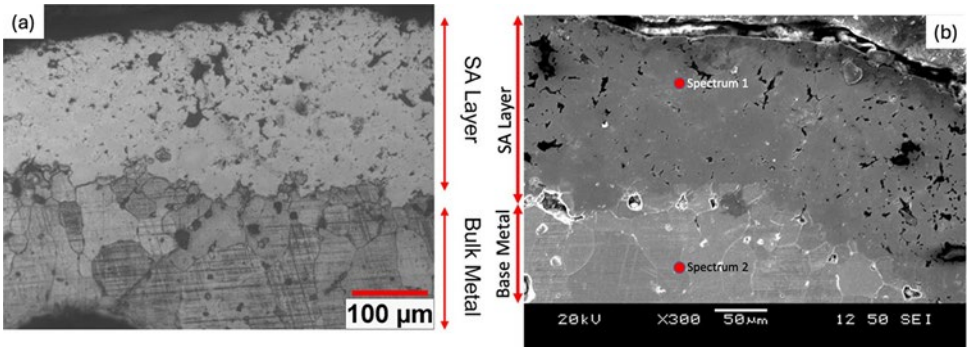

Figure 10. (a) Optical micrograph of S3 casting using alloying element Ni in slurry, showing surface-alloyed layer at 2003, (b) SEM image of sample S3 showing the points where compositional analysis was done.

Table 9. Compositional Analysis of S3 Showing Increased wt% of Ni

Spectrum	Cu (%wt)	Zn (%wt)	Ni (%wt)
Spectrum 1	34.48	3.38	62.14
Spectrum 2	94.40	4.56	1.04

XRD

The X-ray diffraction (XRD) spectra reflect the structure of the surface-alloyed layer since the penetration depth of the X-ray beam is limited to less than 10 lm, and the thickness of the surface-alloyed layer is much greater in all experi- ments. The limited penetration depth of the X-ray beam ensures that the analysis predominantly captures the char- acteristics of the surface layer.

The XRD results of the surface-alloyed Bi-alloy brass samples S3 and S4, shown in Figure 12, reveal the presence of several phases, including Copper–Nickel–Tin, Copper– Nickel–Zinc, and Copper–Zinc solid solutions, as well as pure Ni at 44° and 52°. Similar peaks are seen for the other two samples, S1 and S2, as well. Compared to the base metal, hardly any new crystal peaks are observed in the surface-alloyed layer—which shows that the crystal struc- ture is not drastically altered in this process.

Corrosion Resistance

The corrosion resistance of C89836 in a chloramine environment is greater than that of CuZn40. This improvement is due to the higher concentration of Cu and the addition of Ni as an alloying element in C89836 alloy. The work by Larson et al. demonstrated the beneficial impact of alloying elements such as Ni and Cu on the corrosion resistance of brasses in a chloramine-rich environment. The life of the component increased from 32 days for CuZn40 to 63 days for red brass, which has higher Cu content, to more than 300 days for Monel, which has Ni as the primary element.6 The phase diagram of the Cu–Ni system showed that about 10 wt% Ni can be dissolved in Cu at temperatures up to 1150 °C, which is close to the pouring temperature for brass.

Potentiodynamic tests were conducted on the surface-alloyed samples to test their corrosion rate as compared to the base metal. The tests show a reduction of the corrosion current (Icorr) of the surface-alloyed samples compared to the base metals, as shown in Figure 13. As noted previ- ously, an increase in the amounts of Ni at the surface as a result of surface alloying improves the

corrosion resistance of the sample. The presence of Ni in the surface-alloyed layer has been shown by both SEM-EDS and XRD analysis of the cast surface of the surface-alloyed samples. The surface-alloyed samples show a much lower corrosion current than both the base metals—which is around one- third of the corrosion rate of the base C89836 alloy in tap water, indicating that surface alloying can improve the life of brass components made for the water industry.

Conclusion

The study aimed to enhance the corrosion resistance of yellow brass (CuZn40) and Bi-alloy red brass (C89836) in a chloramine environment through surface alloying, in both laboratory and industrial settings. Surface alloying on selected casting surfaces was achieved by coating the corresponding mold and core surface with slurries containing the alloying powders (Ni, Cu, and Al). Tests were conducted to analyze the chemical composition and corrosion resistance of the surface-alloyed layers on as-cast parts.

These experiments indicated that the surface layers of sand-cast brass components were most effectively enriched using Ni and Cu–Ni powders. A discernible transitional zone was observed between the base metal and the surface- alloyed layer, marked by a decrease in Ni concentration and a corresponding increase in Cu concentration in the base alloy compared to the surface-alloyed layer.

The study also found that melt temperature played a significant role in determining the continuous lengths of the surface-alloyed layer, with higher temperatures resulting in surface-alloyed layers over larger distances. Additionally, corner regions of castings exhibited more pronounced surface alloying due to localized heat zones. In several cases, the formation of porosity was observed within the surface-alloyed layer and at the interface between the base metal and the surface-alloyed layer, which was attributed to gas evolution during melt and metal-binder slurry interaction. The corrosion resistance of the surface-alloyed layer was greater than that of the base metals (both C89836 and CuZn40).

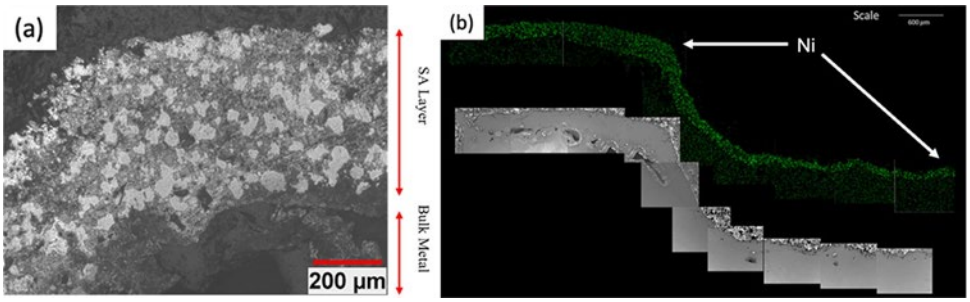

Figure 11. (a) Optical micrograph of sample S4 with Cu-Ni as the powders present in the slurry at 100x, (b) elemental area analysis of sample S4 showing the presence of Ni in the surface-alloyed layer.

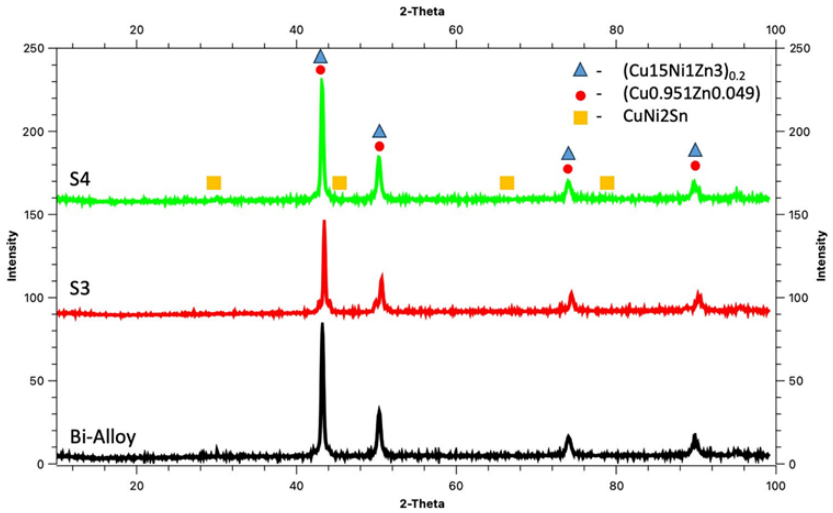

Figure 12. The XRD plots of the base metal Bi-alloy and surface-alloyed samples showing the presence of Ni as a solid solution.

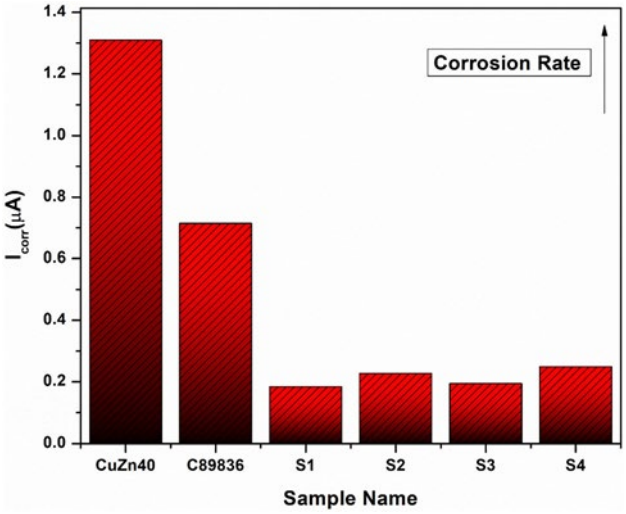

Figure 13. Corrosion resistance of surface-alloyed samples (S1–S4) compared to Bi-alloy.

ACKNOWLEDGEMENTS

The authors are grateful to NSF WEP-I/UCRC for funding the project. They would like to thank Fall River Foundry for providing cores for slurry application, industrial support for casting the C89836 components in their foundry, and the Technikoat mold coating compound. They would like to thank RheoCast foundry for helping cast the Cu60Zn40 alloy. They would also like to thank Vibrantz Technologies and Refcotec for providing the water-based suspending agents and mold coatings used in this study.

This paper is based upon a presentation made in the 2024 AFS Metalcasting Congress. A shortened version was also submitted to the FEF-IJMC Research Competition 2024 by Carol Martinez, who received 1st Place.
Conflict of interest The authors declare no conflict of interest. This research was conducted in the absence of any commercial or financial relationships that could be construed as a potential conflict of interest. All funding sources for this study are acknowledged in the acknowledgments section, and no competing interests influenced the study's design, data collection, interpretation, or decision to publish the results.

REFERENCES

1. J. Choucri, F. Zanotto, V. Grassi, A. Balbo, M. Ebn Touhami, I. Mansouri, C. Monticelli, Corrosion Behavior of different brass alloys for drinking water distribution systems. Metals 9, 649 (2019). https://doi. org/10.3390/met9060649
2. I.K. Marshakov, Corrosion resistance and dezincing of brasses. Prot. Met. 41, 205–210 (2005). https://doi.org/ 10.1007/s11124-005-0031-2
3. M M Al-Abdallah, A K Maayta, M A Al-Qudah, and N A F Al-Rawashdeh Corrosion Behavior of Copper in Chloride Media. (2009). https://doi.org/10.13140/2. 1.1556.4808.
4. O. Kozaderov, K. Shikhaliev, C. Prabhakar, A. Tripathi, D. Shevtsov, A. Kruzhilin, E. Komarova, A. Potapov, I. Zartsyn, Y. Kuznetsov, Corrosion of α-brass in solutions containing chloride ions and 3-mercaptoalkyl-5-amino-1h-1,2,4-triazoles. Appl. Sci. 9, 2821 (2019). https://doi.org/10.3390/ app9142821
5. N.K. Allam, A.A. Nazeer, E.A. Ashour, A review of the effects of benzotriazole on the corrosion of copper and copper alloys in clean and polluted environments. J. Appl. Electrochem. 39, 961–969 (2009). https://doi. org/10.1007/s10800-009-9779-4
6. T.E. Larson, R.M. King, L. Henley, Corrosion of Brass by Chloramine. Journal AWWA 48, 84–88 (1956). https://doi.org/10.1002/j.1551-8833.1956. tb20617.x
7. K. Rane, M. Beining, S. Behera, A. Kordijazi, A. Kumar, P. Rohatgi, Sand casting of surface alloyed butterfly valve with improved hardness and corrosion resistance by incorporating metal powders in-mold coatings. Int. J. Metalcast. 16(1), 359–369 (2022). https://doi.org/10.1007/s40962-021-00609-4
8. Hosmani, S.S., Kuppusami, P., and Goyal, R.K. AnIntroduction to Surface Alloying of Metals Springer India (2014). https://doi.org/10.1007/978-81-322-1889-0
9. K. Rane, S. Behera, A. Kordijazi, P. Rohatgi, Control of thickness and microstructure of surface alloyed layers on mild steels during sand casting. JOM 75, 76–85 (2023). https://doi.org/10.1007/s11837-022-05581-w
10. A. Kordijazi, M. Beining, K. Rane, S. Behera, P. Rohatgi, Surface alloying of internal surfaces of low- carbon steel castings through incorporation of nickel, nickel and chromium, and 316L stainless steel pow- ders to mold and core surfaces. Steel Res. Int. (2022). https://doi.org/10.1002/srin.202100385

11. T.B. Massalski, Phase diagrams in materials science. Metall. Trans. A 20, 1295–1323 (1989). https://doi. org/10.1007/BF02665490
12. Cai, W., Huang, Z., Liu, H., and Liu, R. Effect of Al content on corrosion resistance of Cu-22.7Zn-Al- 1.0Ni brass. In 2011 International Conference on Remote Sensing, Environment and Transportation Engineering IEEE, pp. 3120–3123. (2011). https://doi. org/10.1109/RSETE.2011.5964974.